Characterizing the hypoxic performance of a fish using a new metric: P_{AAS}-50

Yangfan Zhang [a,b*], Daniel W. Montgomery [a], Connor F. White [b], Jeffrey G. Richards [a], Colin J. Brauner [a], Anthony P. Farrell [a]

[a] Department of Zoology and Faculty of Land and Food Systems, University of British Columbia, Vancouver, British Columbia, VT6 1Z4, Canada

[b] Department of Organismic and Evolutionary Biology, Harvard University, 26 Oxford St, Cambridge, Massachusetts, 02138, USA

* Corresponding author. E-mail address: yangfan_zhang@fas.harvard.edu

Keywords: Respirometry, hypoxia, maximum oxygen uptake, aerobic scope, metabolic rate, exercise

Summary statement:

Curvilinear modeling of the limiting effect of oxygen on peak performance of individual fish offers a robust, standardized methodology.

Abstract

The hypoxic constraint on peak oxygen uptake ($\dot{M}O_{2peak}$) was characterized in rainbow trout over a range of ambient oxygen tensions with different testing protocols and statistical models. The best-fit model was selected using both statistical criteria (R^2 & AIC) and the model's prediction of three anchor points for hypoxic performance: critical PO_2 (P_{crit}), maximum $\dot{M}O_2$ and a new metric, the minimum PO_2 that supports 50% of absolute aerobic scope (P_{AAS}-50). The best-fitting model was curvilinear using five

strategically selected PO_2 values. This model predicted P_{AAS}-50 as 70 mm Hg (CV = 9%) for rainbow trout. Thus, while a five-point hypoxic performance curve can characterize the limiting effects of hypoxia in fish, as envisioned by Fry over 75 years ago, P_{AAS}-50 is a promising metric to compare hypoxic constraints on performance in a standardized manner both within and across fish species.

1. Introduction

How an animal's metabolic rate interacts with its ambient environment has long fascinated biologists. For example, characterizing how ambient oxygen constrains whole-organism oxygen uptake ($\dot{M}O_2$) has a long history (Warburg, 1914; Hyman, 1929; Tang, 1933), whether the interest lies with birds flying above the Tibetan Plateau (Black & Tenney, 1980; Lague *et al*., 2017), with mammals living at alpine regions (Terrados *et al*., 1988; Ivy & Scott, 2017), or with fishes exploiting oceanic oxygen minimum zones (Douglas *et al*., 1976) and oxygen-depleted lakes (Lefevre *et al*., 2014). While severely depleted levels of ambient oxygen ultimately constrain an animal's basal or standard metabolic rate (SMR), a less severe level of hypoxia constrains its maximum $\dot{M}O_2$ ($\dot{M}O_{2max}$). For clarity, we define $\dot{M}O_{2max}$ as the highest attainable $\dot{M}O_2$ measured under normoxic conditions and use the term peak $\dot{M}O_2$ ($\dot{M}O_{2peak}$) as the highest attainable $\dot{M}O_2$ measured under all hypoxic conditions. Knowing the exact nature of hypoxia constraint has important physiological and ecological implications because $\dot{M}O_{2peak}$ sets the ceiling for all aerobic activity above SMR. However, measuring $\dot{M}O_{2peak}$ during progressive hypoxia to assess how hypoxia constrains peak aerobic performance is far more technically challenging than measuring routine $\dot{M}O_2$ ($\dot{M}O_{2routine}$). As such, despite its obvious importance, relatively few studies have characterized how hypoxia constrains peak aerobic performance in fish.

In fishes, the limiting effect of declining ambient oxygen levels on the maximum exercise-induced $\dot{M}O_2$ (by critical swim or exhaustive chase protocols), which we collectively term as hypoxic performance models, can take three general forms (Fig. 1A, Fry & Hart, 1948; Neill *et al*., 1994; Claireaux & Lagardère, 1999; Zhang *et al*., 2021). For all these models, one anchor point is $\dot{M}O_{2max}$ and the other is the critical ambient partial pressure of oxygen (PO_2, mm Hg) (P_{crit}). SMR, $\dot{M}O_{2routine}$ and

$\dot{M}O_{2peak}$ of a fish should all converge at P_{crit} (*i.e.*, zero absolute aerobic scope, AAS; Fry & Hart, 1948). In between these two anchor points are three general models. The simplest is a linear model where $\dot{M}O_{2peak}$ conforms with PO_2 (Model I). A partial oxyregulation model (Model II) is where $\dot{M}O_{2peak}$ under modest hypoxic conditions is independent of ambient oxygen and identical to $\dot{M}O_{2max}$ (Fig. 1A & S1), followed by a linear phase of oxyconforming. Model III has two linear phases of oxyconforming. Variations on Models II and III occur when the $\dot{M}O_{2peak}$ dependence on PO_2 is curvilinear (Model IIa & IIIa) rather than linear. A curvilinear model requires more data points to adequately model the hypoxic performance curve relative to a linear model, where a curvilinear model sometimes uses a third value as a reference point. Indeed, curvilinear models could use the midway point between SMR and $\dot{M}O_{2max}$, the minimum PO_2 that would support 50% of AAS (P_{AAS}-50), as a reference point. Regardless of the model, $\dot{M}O_{2peak}$ needs to be repeatedly measured over a range of PO_2 values. It is this challenge that we address here.

Improvements in the techniques and protocols used in aquatic respirometry have done much to pave the way for repeatedly exercising individual fish at multiple levels of hypoxia, which is a requirement for generating a hypoxic performance model. In particular, chasing a fish inside rather than outside a static respirometer allows $\dot{M}O_2$ to be closely monitored during and immediately following exercise, ensuring that $\dot{M}O_{2peak}$ is not missed (Zhang & Gilbert, 2017; Zhang *et al.*, 2020). Analysis of the decline in PO_2 due to fish respiration has also improved. For example, $\dot{M}O_{2peak}$ is estimated more accurately by minimizing the duration of the sampling window for each $\dot{M}O_2$ determination and using an iterative algorithm to specifically identify $\dot{M}O_{2peak}$ (Zhang *et al.*, 2019; Prinzing *et al.*, 2021).

In the present study, we had three objectives. The first was to determine the best statistical model to apply to $\dot{M}O_{2peak}$ data. The second was to define the minimum number of PO_2 values needed for accurate modeling and prediction of P_{AAS}-50. While minimizing the number of PO_2 values reduces the number of separate exercise bouts per fish, the potential confounding effect of cumulative stress, which could reduce $\dot{M}O_{2peak}$, is reduced but not completely eliminated. Therefore, our third objective was to use a control group of fish to independently measure $\dot{M}O_{2max}$ and $\dot{M}O_{2peak}$ at only one level of hypoxia, near the P_{AAS}-50, to determine the degree to which cumulative stress may affect P_{AAS}-50. By satisfying these

objectives we arrived at a recommendation for a testing protocol that reliably quantified the hypoxic performance of individual rainbow trout (*Oncorhynchus mykiss*, Walbaum 1792). This testing protocol advances our ability to capture inter-individual variation relative to an earlier methodology that characterized hypoxic performance in a group of European sea bass (*Dicentrarchus labrax*, Linnaeus, 1758) by chasing different individuals at multiple levels of hypoxia (Claireaux & Lagardère, 1999). Moreover, we generated a reliable estimate of P_{AAS}-50, which has the potential as a standardized metric to compare hypoxic performance within and across fish species.

2. Methods

2.1 Experimental Animals

The experiments were performed on a hatchery-reared, Fraser Valley strain of rainbow trout (*Oncorhynchus mykiss*, Walbaum 1792) (n=23 fish, body mass: 126.4 ± 4.8 g) (Fraser Valley Trout Hatchery, Abbotsford, British Columbia, Canada; Freshwater Fisheries Society of British Columbia). They were held in 200-litre circular tanks containing dechlorinated Vancouver tap water in the Department of Zoology, University of British Columbia (UBC) Aquatics Facility for over 1.5 years prior to experimentation. Monitoring of water temperature (11 °C for at least three months before experimentation started) and fish feeding (a maintenance ration, 1% body mass, of commercial trout pellets, Skretting Canada Inc., Vancouver, BC, Canada) were performed daily. Animal holding and experimental procedures were approved by The UBC Animal Care Committee (A18-0340).

2.2 Respirometry apparatus

The hypoxic performance trials were conducted on individual fish (fasted for 48h) placed into one of four replicated 4.1-litre Loligo-type, static respirometers (water volume to fish mass ratio of about 33:1, Loligo Systems, Tjele, Denmark). Fish were habituated to normoxic conditions with the respirometer in a water flush mode for at least 30 mins before the first chase (see below) to assure that fish at least repaid

the high-energy phosphate and oxygen stores that might be somewhat consumed during handling (Zhang *et al*., 2018). The respirometers were submerged in a water table (2.4 × 0.8 × 0.4 m) filled with fully aerated freshwater, which accommodated all four respirometers and allowed simultaneous measurements on four individuals. A water temperature regulator (Ecoplus ¼ HP chiller, Vancouver, USA) maintained the temperature of the water table at 11 °C and circulated the contents of the water table. The entire respirometry system was located inside a thermally regulated (11 °C) environmental chamber. The water volume of the entire system was replaced in between trials. Every five days, the entire respirometry system was disinfected with Virkon Aquatic (10 g l^{-1}; Syndel Canada), rinsed thoroughly, and the water in the respirometers and water table replaced.

The water from the water table was intermittently circulated through each respirometer using individual, computer-controlled (AquaResp v.3, Aquaresp.com, Denmark) flush pumps (Universal 3400, EHEIM, Deizisau, Germany). Flush pumps were stopped at the beginning of each 600-s $\dot{M}O_2$ monitoring period (AquaResp v.3, Denmark, Aquaresp.com), which was followed by 30-s flushing and 40-s equilibration periods. Each respirometer also had a recirculation loop which contained a dedicated external pump (Universal 600, EHEIM, Deizisau, Germany) and an optical oxygen probe (Robust Oxygen Probe OXROB10) to continuously record the oxygen partial pressure (PO_2, mm Hg) of ambient water inside the respirometer (recording frequency ~1 Hz, response time < 15 s, PyroScience GmbH, Germany). Oxygen probes were calibrated to 0 mm Hg (0 kPa, water saturated with sodium sulphite and bubbled with nitrogen gas) and fully aerated water (157 mm Hg = 20.9 kPa,). The background $\dot{M}O_2$ in each respirometer was measured for 25 min after each trial had been completed. In the few occasions where background exceeded 1% of $\dot{M}O_{2routine}$, a correction was applied to the $\dot{M}O_2$ measurement.

Each respirometer was equipped with a chasing device (a soft piece of 25-cm cable tie attached to a 20 cm metal stem bent at a right angle and inserted through a 1.5-cm diameter sealed port located mid-way along the top of the respirometer, Zhang *et al*., 2020), which when repeatedly turned from the outside would agitate the fish to perform C-start turns until it fatigued.

2.3 Assessment of hypoxic performance

Modeling hypoxic performance above the P_{crit} (17.6 mm Hg or 2.3 kPa; see below) required a preliminary trial (n=3 fish) to strategically select the ambient PO_2 test range to bracket the anticipated P_{AAS}-50, much like acute toxicity testing brackets median lethal concentrations. Based on these preliminary data, three testing protocols (four-point, five-point and seven-point PO_2 levels) were designed (n=7-8 fish for each protocol): the four-point model used PO_2 levels of 142, 96, 70 & 41 mm Hg (18.9, 12.8, 9.3 & 5.5 kPa), the five-point model used PO_2 levels of 141, 103, 86, 72 & 40 mm Hg (18.8, 13.7, 11.5, 9.6 & 5.3 kPa) and the 7-point model used PO_2 levels of at 142, 110, 97, 84, 69, 57 & 41 mm Hg (18.9, 14.7, 12.9, 11.2, 9.2, 7.6 & 5.5 kPa) (all values are the mean value for the mid-point of the ambient PO_2 while the respirometer was closed). Each testing protocol involved a stepwise deoxygenation of the respirometers with an $\dot{M}O_{2peak}$ determination (described below) at each PO_2 level. Thus, the three testing protocols all started with an $\dot{M}O_{2peak}$ at normoxia for each fish and then examined either 3, 4 or 6 levels of hypoxia for that fish.

$\dot{M}O_{2peak}$ was measured at each of these PO_2 levels by turning off the flush plumps and sealing the respirometer. The fish was then individually exercised to fatigue by rapidly turning the chasing devise for 5 min, after which it was left undisturbed for 5 min to capture the initial portion of the excess post-exercise oxygen consumption (EPOC; Fig. 2), *i.e.*, a closed monitoring cycle of 10 min. Subsequent off-line analysis captured the highest $\dot{M}O_2$ values during this 10-min $\dot{M}O_2$ monitoring period, and $\dot{M}O_{2peak}$ was assigned to the highest of these values (*see* below & representative individual traces in Fig. S1), and the associated PO_2 is peak PO_2 (PO_{2peak}; see calculation in section 2.5.1 & values in Fig. 1 & 3). At the end of each 10-min $\dot{M}O_2$ monitoring period, the respirometer flush pumps were turned on to introduce hypoxic water into the respirometer and gradually achieve one of the predetermined PO_2 levels outlined above using a four-min cycling of a 30 s flushing period, a 40 s equilibration period and a 170 s $\dot{M}O_2$ monitoring period. Hypoxic water was generated using a custom-built, 10-l gas equilibration column situated upstream of the water table (it received the normoxic water at the top and nitrogen gas was injected at the bottom) and reduced the water PO_2 of the entire respirometry system. This exercise protocol was repeated

at each PO_2 test level. Thus, each 10-min period when a fish was exercised and began recovery was followed by a 20-min recovery period during which $\dot{M}O_2$ was monitored on-line (data not presented). This same protocol was followed for each PO_2 test level except the final one (39–42 mm Hg or 5.2–5.6 kPa), which required a little longer degassing period (~30 min) to reach the desired ambient PO_2. At the end of the trial, the fish were removed from their respirometers and returned to three holding tanks where the four-, five- and seven-point test groups were kept separated. After a 10-day recovery, the same fish from the five-point or seven-point test groups were re-tested to check the repeatability of the five-point and seven-point data. The four-point protocol was not repeated after it produced an inferior hypoxic performance curve – see Results. Additional details concerning the respirometry system and the testing protocols are available in Table S1 in Zhang *et al.*, 2022.

2.4 Independent measurements of SMR, P_{crit} and $\dot{M}O_{2peak}$ in normoxia and near P_{AAS}-50.

SMR, $\dot{M}O_{2peak}$ in normoxia and $\dot{M}O_{2peak}$ at P_{AAS}-50 were independently measured on a group of 8 naïve fish using the same test apparatus, measurement protocols and chasing protocols as described above. In contrast, once $\dot{M}O_{2peak}$ was measured in normoxia, the fish were left undisturbed in the respirometer that was continuously flushed with normoxic water for a 2-day quiescent period during which $\dot{M}O_{2routine}$ was continuously measured and SMR was estimated from these measurements (see below). After this quiescent period, the water was gradually deoxygenated at a similar rate (total time ~ 50 min) to near the P_{AAS}-50 estimated from the hypoxic performance curve (around 75 mm Hg = 9.9 kPa,), at which another $\dot{M}O_{2peak}$ determination was made as described above. These estimates of $\dot{M}O_{2peak}$ in normoxia and at P_{AAS}-50 were statistically compared with those obtained with the hypoxic performance testing protocol to examine whether cumulative exercise in hypoxia affected these estimates. SMR was statistically compared with an independent measurement of SMR from another group of eight naïve fish that were never chased. These additional fish were placed into the respirometers and left undisturbed under normoxic conditions for a similar 2-day quiescent period during which $\dot{M}O_{2routine}$ was continuously

measured to determine SMR. After this quiescent period, a well-established hypoxia challenge test (Claireaux *et al*., 2013) was performed to provide an estimate of P_{crit} (Claireaux & Chabot, 2016).

2.5 Data analysis

2.5.1 $\dot{M}O_2$, $\dot{M}O_{2peak}$ and SMR analyses

$\dot{M}O_2$ values (mg O_2 h^{-1} kg^{-1}) at each ambient water PO_2 level were determined with off-line analysis of the continuous measurement of the declining water PO_2 when the respirometer was closed during a measurement cycle. An iterative algorithm (Eqn.1) was applied (Zhang *et al*., 2019), one that slides a minimum sampling window duration as a rolling regression through the continuous, 10-min PO_2 trace. A minimum sampling window duration for a reliable $\dot{M}O_2$ determination was 100 s, based on an analysis of eight background $\dot{M}O_2$ traces (Fig. S2). $\dot{M}O_{2peak}$ was defined as the highest $\dot{M}O_2$ attained during a 5-min chase of fish inside the static respirometer (higher values were not obtained during EPOC, Fig. 2, Fig. S1). The PO_{2peak} was the mid-point of the PO_2 slope used for this $\dot{M}O_{2peak}$ determination. On-line reporting of $\dot{M}O_2$ (set by AquaResp v.3 software) was only used for monitoring purposes.

$$\text{Peak } \dot{M}O_2 = \max\left\{\left[\frac{d_{DO[n,(n+a)]}}{d_{t[n,(n+a)]}} * \left(V_r - V_f\right) * S_O\right] / (t * M_f)\right\} \qquad \text{Rolling regression analysis (Eqn. 1)}$$

$$\dot{M}O_2 = \left[\frac{d_{DO[i,(i+a)]}}{d_{t[i,(i+a)]}} * \left(V_r - V_f\right) * S_O\right] / (t * M_f) \qquad \text{Sequential interval regression analysis (Eqn. 2)}$$

Where d_{DO}/d_t is the change in O_2 saturation with time, V_r is the respirometer volume, V_f is the fish volume (1 g body mass = 1 ml water), S_o is the water solubility of O_2 (calculated by AquaResp v.3 software) at the experimental temperature, salinity and atmospheric pressure, t is a time constant of 3600 s h^{-1}, M_f is fish mass, n is one PO_2 sample forward from the 1st PO_2 recorded in the sealed respirometer, and

a is the sampling window duration of 100 s., *i* is the next PO_2 sample after the preceding sampling window.

SMR was estimated from ~288 $\dot{M}O_2$ calculations using Eqn. 2 collected during a 2-day quiescent period in the respirometer and applying a 20th quantile algorithm (Chabot *et al*., 2016; Chabot *et al*., 2021).

P_{crit} was estimated by fitting a linear regression function of ambient water PO_2 to the declining $\dot{M}O_2$ (calculated using Eqn. 2) during the final stages of the hypoxia challenge test. P_{crit} was assigned to the PO_2 by solving this regression for SMR (Claireaux & Chabot, 2016), *i.e*., the intersection of the regression line with SMR (Fig. 1).

2.5.2 Statistical modeling of hypoxic performance: $\dot{M}O_{2peak}$ as a function of ambient PO_2

The responses of $\dot{M}O_{2peak}$ (y) as a function of ambient water PO_2 (x) were statistically modeled with both a linear regression equation (Eqn. 3) and an asymptotic equation (Eqn. 4) (Mueller & Seymour 2011). The quality of these statistical fits for the four-point, five-point and seven-point data sets was assessed by least-squares regressions following Akaike information criterion (AIC) (*see* model parameters in Table S2 in Zhang *et al*., 2022).

$y = a * x + b$ Linear regression equation (Eqn. 3)

Where *a* is the slope, a rate constant for a linear increase, *b* is the intercept at the y-axis.

$$y = Asymptote\left(1 - e^{-e^{K}(x-I)}\right)$$

Asymptotic equation (Eqn. 4)

Where *I* is the intercept at the x-axis, *Asymptote* is a line that the curve continues to approach at infinity. *Asymptote* is expressed in the same unit as y. *I* is expressed in the same unit as x. *K* is the rate constant.

The repeatability of the five-point and seven-point hypoxic performance models was statistically tested by comparing the 1st and 2nd determinations using a non-linear mixed-effects model (Eqn. 5) (lmerTest package in R v.4.1.1).

$$y = (Asymptote + a)\left(1 - e^{-e^{K+b}(x-I+c)}\right)$$

Reproducibility test for asymptotic equation (Eqn. 5)

Where *a*, *b*. *c* are the respective modifiers for the *Asymptote*, rate constant for a hyperbolic increase (*K*), and intercept (*I*) for the 2nd hypoxic performance test (Eqn. 5). If the modifiers reached statistical significance ($\alpha < 0.05$), the two asymptotic equations were deemed different.

P_{AAS}-50 was estimated by normalizing individual $\dot{M}O_{2peak}$ values to a percentage of their individual AAS (AAS = $\dot{M}O_{2max}$ – SMR) and interpolating P_{AAS}-50 as the minimum PO_2 supporting the 50% of AAS from the best-fitted hypoxic performance model. The extrapolated SMR values were calculated based on P_{crit} using the best-fitted hypoxic performance model.

2.5.3 Statistical analysis

Measurements points were presented as mean ± s.e.m. for $\dot{M}O_{2peak}$ and PO_{2peak}, and 95% C.I. was provided for the hypoxic performance equations. Logarithm transformations were applied on the metrics that failed normality tests to meet the assumptions of normality of residuals, homoscedasticity of the residuals and no trend in the explanatory variables. Statistical comparisons among different individuals, and for measured and extrapolated $\dot{M}O_2$ values used one-way ANOVA with Holm-Šídák *post-hoc* tests. The comparisons of the same individuals used paired t-tests. The statistical analyses were conducted in SPSS v.26 (SPSS Inc. Chicago, IL, USA). The best-fitting regression analyses were conducted using Prism v.9 (GraphPad Software, San Diego, CA, USA). Significances were assigned when $\alpha < 0.05$. Analysis of the

respirometry data was performed in R v.4.1.1 software and R studio (RStudio team, 2021) using either the fishMO2 package (Claireaux & Chabot, 2016), or LabChart v.8.0 (ADInstruments, Colorado Springs, CO, USA).

3. Results and Discussion

$\dot{M}O_{2peak}$ was typically reached during the chase (sometimes more than once), but rarely during the EPOC period (Fig. 2; Figs. S1-S3). While $\dot{M}O_2$ typically declined exponentially when PO_2 was above ~100 mm Hg, $\dot{M}O_2$ remained quite constant during EPOC below ~70 mm Hg (Fig. 2). Thus, we confirm that chasing fish inside a respirometer provides a more reliable measurement of $\dot{M}O_{2peak}$ than quickly transferring an exhausted fish into a respirometer and measuring $\dot{M}O_2$ during the initial phase of EPOC (Zhang *et al*., 2020). Thus, a key criterion of measuring $\dot{M}O_{2peak}$ is that a sustained workload on an individual is a prerequisite of a sustained peak performance (Midgley *et al*., 2007; Copp *et al*., 2009). In addition, we confirmed the normoxic anchor points by showing that an independently measured $\dot{M}O_{2peak}$ at normoxia was indistinguishable from that determined with the hypoxic performance protocol (F = 0.574, p = 0.637, power = 0.662; Fig. 1, Fig. S3).

We rejected Model I for the rainbow trout and compared a two-segmented linear regression model with an asymptotic model for the best statistical fit. The former is often used to evaluate the dependence of $\dot{M}O_{2routine}$ on PO_2 (Ultsch *et al*., 1980), while both models are used for hypoxic performance modeling (Mueller & Seymour, 2011). An asymptotic equation (curvilinear) modeled the hypoxic performance of rainbow trout no better than a linear regression equation based on AIC (AIC = four-point: 287.8 vs 286.7, five-point: 378.0 vs 381.9, seven-point: 513.8 vs 517.7) and only marginally better based on R^2 (R^2 = four-point: 0.900 vs 0.897, five-point: 0.936 vs 0.926; seven-point: 0.954 vs 0.949) (Fig. 1; Table S2 in Zhang *et al*., 2022). However, the curvilinear model was superior to the linear regression in terms of predicting the second anchor point of hypoxic performance, SMR; solving and extrapolating the linear models for the independently measured P_{crit} (17.6 ± 0.9 mm Hg., Fig. 1b, c) consistently overestimated SMR (76.0–90.9 mg O_2 h^{-1} kg^{-1}) by a very large amount (74–143%) compared

with the independently measured SMR value (SMR = 43.9 mg O_2 h^{-1} kg^{-1}; $F = 46.85$, $p < 0.0001$; Fig. 1). In contrast, extrapolation of the five- and seven-point asymptotic equations (35.1 ± 3.8 & 43.4 ± 3.8 mg O_2 h^{-1} kg^{-1}, $F = 2.3$, $p = 0.12$, power = 0.394; Fig. 1) reliably predicted the measured SMR. Thus, using either five or seven strategically selected PO_2 values with an asymptotic equation generated a reliable characterization of the hypoxic performance curve for rainbow trout, one that accurately predicted SMR using a known P_{crit}. However, we rejected a four-point curvilinear model because it also overestimated SMR by 50% (SMR = 65.6 mg O_2 h^{-1} kg^{-1} $F = 38.11$, $p < 0.001$) despite a good statistical fit ($R^2 = 0.900$; AIC = 287.8).

We proposed P_{AAS}-50 as a potential third anchor point of a hypoxic performance curve. P_{AAS}-50 interpolations were statistically indistinguishable ($t = 0.10$, $p = 0.92$, power = 0.051) for the five-point (1st test= 71.6 ± 2.3, 2nd test = 68.8 ± 2.2 mm Hg) and seven-point (1st test = 72.1 ± 4.2, 2nd test = 68.2 ± 1.5 mm Hg) curvilinear models. Also, the interpolated $\dot{M}O_{2peak}$ values at P_{AAS}-50 were indistinguishable from the independent measurements ($F = 2.047$, $p = 0.131$, power = 0.466; Fig. 1, Fig. S3). Consequently, five strategically selected PO_2 levels are likely the minimum number of data points needed to reliably model a hypoxic performance curve and predict P_{AAS}-50. Nevertheless, further studies are needed to understand whether a curvilinear or a linear model applies to the hypoxic performance of other fish species.

The reproducibility of the five-point and seven-point hypoxic performance curve protocols was confirmed by retesting the same individuals after a 10-day recovery period. The re-tested five-point hypoxic performance curve only manifested the slower rate of decline than the first test ($t = 2.49$, $p = 0.015$; Table S3 in Zhang *et al*., 2022; Fig. 3) whereas the re-tested seven-point hypoxic performance curve manifested a slower rate of decline (*i.e.* the lower tangent; $t = 2.49$, $p = 0.015$) and a lower asymptote ($t = 2.07$, $p = 0.04$) than the first test. Consequently, $\dot{M}O_{2peak}$ at normoxia for the re-tested five-point hypoxic performance curve was only 9% lower than the first test ($t = 2.86$, $p = 0.024$, Fig. 3) and 12% lower with the re-tested seven-point hypoxic performance curve. $\dot{M}O_{2peak}$ for the re-tested five-point hypoxic performance had an 8% lower $\dot{M}O_{2peak}$ at 85 mm Hg ($t \geq 4.05$, $p \leq 0.007$) than the first test.

Despite the inconsequential difference in the $\dot{M}O_{2peak}$ values, P_{AAS}-50 values for the re-tests were indistinguishable from those of the first tests (t = 0.22, p = 0.82, power = 0.055) (Fig. 3).

The consistent values for $\dot{M}O_{2peak}$ at P_{AAS}-50 by independent means suggest that the cumulative stress associated with repeat chasing to fatigue did not impact this variable. This finding implies that rainbow trout exercised to fatigue for 5 min and allowed to recover for 25 min can repeat their peak performance even though the fish only partially repaid their EPOC. Indeed, exhausted salmonids take about 30 min to replenish the majority of their oxygen stores and high energy phosphate (Wood, 1991; Scarabello *et al*., 1991; Scarabello *et al*., 1992; Zhang *et al*., 2018) and salmonids can repeat a critical swimming test after just a 20–40 min recovery from the fatigue experienced in the previous test while carrying some unpaid EPOC (Randall *et al*., 1987; Jain *et al*., 1997; Jain *et al*., 1998; Farrell *et al*., 1998; Farrell *et al*., 2001; Wagner *et al*., 2006; Steinhausen *et al*., 2008). Likewise, European sea bass (*Dicentrarchus labrax*) repeated four constant acceleration tests with only a 5-min rest period between tests (Marras *et al*., 2010). Whether or not other fish species can repeat perform as quickly remains to be determined.

The low coefficient of variation for the P_{AAS}-50 (<10% for both five-point determinations) suggests that it may be a robust and potentially valuable metric to compare hypoxic performance curves across fish species or within a species across different ambient environments. Also, it is tempting to suggest that the curvilinear nature of the rainbow trout hypoxic performance curve reflects the sigmoidal shape of the blood oxygen equilibrium curve (Weber *et al*., 1987). However, the P_{AAS}-50 was around 70 mm Hg, which is approximately twice the P_{50} of exercised rainbow trout hemoglobin (~35 mm Hg; Rummer & Brauner, 2015). Therefore, other physiological factors must affect the positioning of the curvilinear hypoxic performance of rainbow trout.

What is clear from our data, however, is that a linear model is inaccurate over a wide range of PO_2 values. A linear model with the anchor points of P_{crit} and the zero intercept for $\dot{M}O_2$ and PO_2 has been used in a different context to describe hypoxic performance (Seibel *et al*., 2021). However, all our hypoxic performance curve models had non-zero intercepts (Table S2 in Zhang *et al*., 2022 & Fig. 1B &

1C), suggesting that forcing the intercept through the origin lacks biological relevance, at least in trout. Moreover, such a linear model was suggested to be able to predict $\dot{M}O_{2max}$ (Seibel *et al*., 2021), presumably at normoxia. However, this extrapolation for our measured P_{crit} in rainbow trout predicted a $\dot{M}O_{2max}$ that was 13% lower (t = 2.73, p = 0.009; 357 mg O_2 h^{-1} kg^{-1}) than our measured value. While such a difference can be considered small, larger differences might be expected when such extrapolations are made for fishes with a lower P_{crit} than rainbow trout. In particular, the linear extrapolation through the origin for the measured P_{crit} value in European sea bass (*Dicentrarchus labrax*) (Zhang, 2021) predicted a $\dot{M}O_{2max}$ that was 47% higher than that measured (t = 12.7, p < 0.0001). Thus, any such linear models and extrapolations should be conducted with caution.

In conclusion, the hypoxic performance curve protocol provides a respiratory phenotyping platform to compare fish's ability to exercise under hypoxia. We recommend the five-point hypoxic performance curve as a reliable, time-efficient and reproducible methodology to functionally quantify the hypoxic performance of individual fish and for interpolation of the P_{AAS}-50, which may prove to be a valuable comparative tool for hypoxic performance both within and across species. Zoologists can now measure the limiting effects of hypoxia in fish that is envisioned by Fry over 75 years ago.

Ethics. Fish holding and all experimental procedures were approved by the University of British Columbia Animal Care Committee (A18-0340).

Authors' contributions. Y.Z., A.P.F. conceived and designed the experiments. Y.Z. conducted the respirometry experiment, data analysis and wrote the manuscript. D.M. assisted with the respirometry experiments and respirometry data acquisition. C.W. assisted in data analysis. C.B., J.R. greatly contribute to all aspects of the project. A.P.F. collaborated in editing the manuscript. All authors read, contributed to, and approved the final manuscript.

Acknowledgements. The author particularly appreciates the numerous insightful discussions with Dr. Guy Claireaux and Dr. Denis Chabot over the years. We appreciate the logistical assistance from Dr. Phillip Morrison and staff in the aquatic facility and workshop at the Department of Zoology, the University of British Columbia. We appreciate the constructive feedback provided by two anonymous reviewers.

Funding. This work was supported by British Columbia Salmon Restoration and Innovation Fund (BCSRIF-083) awarded to J.G.R. & C.J.B.. A.P.F. holds an NSERC Discovery Grant and a Canada Research Chair Tier I. Y.Z. holds an NSERC Postdoctoral Fellowship.

Data accessibility. All data are provided within the manuscript itself or the electronic supplementary material. Further information available upon request.

Conflict of Interest. The authors declare that they have no competing interests.

References

Black, C. P., & Tenney, S. M. (1980). Oxygen transport during progressive hypoxia in high-altitude and sea-level waterfowl. *Respiration Physiology*, *39*(2), 217–239. https://doi.org/10.1016/0034-5687(80)90046-8

Chabot, D., Steffensen, J. F., & Farrell, A. P. (2016). The determination of standard metabolic rate in fishes. *Journal of Fish Biology*, *88*(1), 81–121. https://doi.org/10.1111/jfb.12845

Chabot, D., Zhang, Y., & Farrell, A. P. (2021). Valid oxygen uptake measurements: Using high r2 values with good intentions can bias upward the determination of standard metabolic rate. *Journal of Fish Biology*, *98*(5), 1206–1216. https://doi.org/10.1111/jfb.14650

Claireaux, G., & Chabot, D. (2016a). Responses by fishes to environmental hypoxia: Integration through Fry's concept of aerobic metabolic scope. *Journal of Fish Biology*, *88*(1), 232–251. https://doi.org/10.1111/jfb.12833

Claireaux, G., & Chabot, D. (2016b). Responses by fishes to environmental hypoxia: Integration through Fry's concept of aerobic metabolic scope. *Journal of Fish Biology*, *88*(1), 232–251. https://doi.org/10.1111/jfb.12833

Claireaux, G., & Lagardère, J.-P. (1999). Influence of temperature, oxygen and salinity on the metabolism of the European sea bass. *Journal of Sea Research*, *42*(2), 157–168. https://doi.org/10.1016/S1385-1101(99)00019-2

Claireaux, G., Théron, M., Prineau, M., Dussauze, M., Merlin, F.-X., & Le Floch, S. (2013). Effects of oil exposure and dispersant use upon environmental adaptation performance and fitness in the European sea bass, Dicentrarchus labrax. *Aquatic Toxicology*, *130–131*, 160–170. https://doi.org/10.1016/j.aquatox.2013.01.004

Copp, S. W., Davis, R. T., Poole, D. C., & Musch, T. I. (2009). Reproducibility of endurance capacity and VO2peak in male Sprague-Dawley rats. *Journal of Applied Physiology (Bethesda, Md.: 1985)*, *106*(4), 1072–1078. https://doi.org/10.1152/japplphysiol.91566.2008

Douglas, E. L., Friedl, W. A., & Pickwell, G. V. (1976). Fishes in oxygen-minimum zones: blood oxygenation characteristics. *Science*, *191*(4230), 957–959. https://doi.org/10.1126/science.1251208

Farrell, A. P., Gamperl, A. K., & Birtwell, I. K. (1998). Prolonged swimming, recovery and repeat swimming performance of mature sockeye salmon Oncorhynchus nerka exposed to moderate hypoxia and pentachlorophenol. *Journal of Experimental Biology*, *201*(14), 2183–2193. https://doi.org/10.1242/jeb.201.14.2183

Fry, F. E. J., & Hart, J. S. (1948). The relation of temperature to oxygen consumption in the goldfish. *The Biological Bulletin*, *94*(1), 66–77. https://doi.org/10.2307/1538211

Hyman, L. H. (1929). The effect of oxygen tension on oxygen consumption in planaria and some echinoderms. *Physiological Zoology*, *2*(4), 505–534. https://doi.org/10.1086/physzool.2.4.30152973

Ivy, C. M., & Scott, G. R. (2017). Control of breathing and ventilatory acclimatization to hypoxia in deer mice native to high altitudes. *Acta Physiologica (Oxford, England)*, *221*(4), 266–282. https://doi.org/10.1111/apha.12912

Jain, K. E., Birtwell, I. K., & Farrell, A. P. (1998). Repeat swimming performance of mature sockeye salmon following a brief recovery period: A proposed measure of fish health and water quality. *Canadian Journal of Zoology*, *76*(8), 1488–1496. https://doi.org/10.1139/z98-079

Jain, K. E., Hamilton, J. C., & Farrell, A. P. (1997). Use of a ramp velocity test to measure critical swimming speed in rainbow trout (*Onchorhynchus mykiss*). *Comparative Biochemistry and Physiology Part A: Physiology*, *117*(4), 441–444. https://doi.org/10.1016/S0300-9629(96)00234-4

Lague, S. L., Chua, B., Alza, L., Scott, G. R., Frappell, P. B., Zhong, Y., Farrell, A. P., McCracken, K. G., Wang, Y., & Milsom, W. K. (2017). Divergent respiratory and cardiovascular responses to hypoxia in bar-headed geese and Andean birds. *Journal of Experimental Biology*, *220*(22), 4186–4194. https://doi.org/10.1242/jeb.168799

Lefevre, S., Damsgaard, C., Pascale, D. R., Nilsson, G. E., & Stecyk, J. A. W. (2014). Air breathing in the Arctic: Influence of temperature, hypoxia, activity and restricted air access on respiratory physiology of the Alaska blackfish Dallia pectoralis. *Journal of Experimental Biology*, *217*(24), 4387–4398. https://doi.org/10.1242/jeb.105023

Marras, S., Claireaux, G., McKenzie, D. J., & Nelson, J. A. (2010). Individual variation and repeatability in aerobic and anaerobic swimming performance of European sea bass, Dicentrarchus labrax. *Journal of Experimental Biology*, *213*(1), 26–32. https://doi.org/10.1242/jeb.032136

Midgley, A. W., McNaughton, L. R., & Carroll, S. (2007). Reproducibility of time at or near VO2max during intermittent treadmill running. *International Journal of Sports Medicine*, *28*(1), 40–47. https://doi.org/10.1055/s-2006-923856

Mueller, C. A., & Seymour, R. S. (2011). The regulation index: A new method for assessing the relationship between oxygen consumption and environmental oxygen. *Physiological and Biochemical Zoology: PBZ*, *84*(5), 522–532. https://doi.org/10.1086/661953

Neill, W. H., Miller, J. M., Van Der Veer, H. W., & Winemiller, K. O. (1994). Ecophysiology of marine fish recruitment: A conceptual framework for understanding interannual variability. *Netherlands Journal of Sea Research*, *32*(2), 135–152. https://doi.org/10.1016/0077-7579(94)90037-X

Prinzing, T. S., Zhang, Y., Wegner, N. C., & Dulvy, N. K. (2021). Analytical methods matter too: Establishing a framework for estimating maximum metabolic rate for fishes. *Ecology and Evolution*, *00*, 1–17. https://doi.org/10.1002/ece3.7732

Randall, D. J., Mense, D., & Boutilier, R. G. (1987). The effects of burst swimming on aerobic swimming in chinook salmon (*Oncorhynchus tshawytscha*). *Marine Behaviour and Physiology*, *13*(1), 77–88. https://doi.org/10.1080/10236248709378664

Rummer, J. L., & Brauner, C. J. (2015). Root effect haemoglobins in fish may greatly enhance general oxygen delivery relative to other vertebrates. *PLOS ONE*, *10*(10), e0139477. https://doi.org/10.1371/journal.pone.0139477

Scarabello, M., Heigenhauser, G. J., & Wood, C. M. (1992). Gas exchange, metabolite status and excess post-exercise oxygen consumption after repetitive bouts of exhaustive exercise in juvenile rainbow trout. *Journal of Experimental Biology*, *167*(1), 155–169. https://doi.org/10.1242/jeb.167.1.155

Scarabello, M., Wood, C., & Heigenhauser, G. (1991). Glycogen depletion in juvenile rainbow trout as an experimental test of the oxygen debt hypothesis. *Canadian Journal of Zoology*, *69*(10), 2562–2568. https://doi.org/10.1139/z91-361

Seibel, B. A., Andres, A., Birk, M. A., Burns, A. L., Shaw, C. T., Timpe, A. W., & Welsh, C. J. (2021). Oxygen supply capacity breathes new life into critical oxygen partial pressure (Pcrit). *Journal of Experimental Biology*, *224*(8). https://doi.org/10.1242/jeb.242210

Steinhausen, M. F., Sandblom, E., Eliason, E. J., Verhille, C., & Farrell, A. P. (2008). The effect of acute temperature increases on the cardiorespiratory performance of resting and swimming sockeye salmon (*Oncorhynchus nerka*). *Journal of Experimental Biology*, *211*(24), 3915–3926. https://doi.org/10.1242/jeb.019281

Tang, P.-S. (1933). On the rate of oxygen consumption by tissues and lower organisms as a function of oxygen tension. *The Quarterly Review of Biology*, *8*(3), 260–274.

Terrados, N., Melichna, J., Sylvén, C., Jansson, E., & Kaijser, L. (1988). Effects of training at simulated altitude on performance and muscle metabolic capacity in competitive road cyclists. *European Journal of Applied Physiology and Occupational Physiology*, *57*(2), 203–209. https://doi.org/10.1007/BF00640664

Ultsch, G. R., Ott, M. E., & Heisler, N. (1980). Standard metabolic rate, critical oxygen tension, and aerobic scope for spontaneous activity of trout (*Salmo gairdneri*) and carp (*Cyprinus carpio*) in acidified water. *Comparative Biochemistry and Physiology Part A: Physiology*, *67*(3), 329–335. https://doi.org/10.1016/S0300-9629(80)80004-1

Wagner, G. N., Kuchel, L. J., Lotto, A., Patterson, D. A., Shrimpton, J. M., Hinch, S. G., & Farrell, A. P. (2006). Routine and active metabolic rates of migrating adult wild sockeye salmon (*Oncorhynchus nerka* Walbaum) in Seawater and Freshwater. *Physiological and Biochemical Zoology: Ecological and Evolutionary Approaches*, *79*(1), 100–108. https://doi.org/10.1086/498186

Warburg, O. (1914). Beiträge zur Physiologie der Zelle, insbesondere über die Oxydationsgeschwindigkeit in Zellen. *Ergebnisse der Physiologie*, *14*(1), 253–337. https://doi.org/10.1007/BF02188636

Weber, R. E., Jensen, F. B., & Cox, R. P. (1987). Analysis of teleost hemoglobin by Adair and Monod-Wyman-Changeux models. *Journal of Comparative Physiology B*, *157*(2), 145–152. https://doi.org/10.1007/BF00692358

Wood, C. M. (1991). Acid-Base and ion balance, metabolism, and their interactions, after exhaustive exercise in fish. *Journal of Experimental Biology*, *160*(1), 285–308. https://doi.org/10.1242/jeb.160.1.285

Zhang, Y. (2021). Interpreting species, intraspecific and intra-individual variability by comprehensively characterizing a fish's respiratory phenotype with valid measures of oxygen uptake [University of British Columbia]. https://doi.org/10.14288/1.0396683

Zhang, Y., Claireaux, G., Takle, H., Jørgensen, S. M., & Farrell, A. P. (2018). A three-phase excess post-exercise oxygen consumption in Atlantic salmon *Salmo salar* and its response to exercise training. *Journal of Fish Biology*, *92*(5), 1385–1403. https://doi.org/10.1111/jfb.13593

Zhang, Y., & Gilbert, M. J. H. (2017). Comment on 'Measurement and relevance of maximum metabolic rate in fishes by Norin & Clark (2016).' *Journal of Fish Biology*, *91*(2), 397–402. https://doi.org/10.1111/jfb.13291

Zhang, Y., Gilbert, M. J. H., & Farrell, A. P. (2019). Finding the peak of dynamic oxygen uptake during fatiguing exercise in fish. *Journal of Experimental Biology*, *222*(12). https://doi.org/10.1242/jeb.196568

Zhang, Y., Gilbert, M. J. H., & Farrell, A. P. (2020). Measuring maximum oxygen uptake with an incremental swimming test and by chasing rainbow trout to exhaustion inside a respirometry chamber yields the same results. *Journal of Fish Biology*, *97*(1), 28–38. https://doi.org/10.1111/jfb.14311

Zhang, Y., So, B. E., & Farrell, A. P. (2021). Hypoxia performance curve: Assess a whole-organism metabolic shift from a maximum aerobic capacity towards a glycolytic capacity in fish. *Metabolites*, *11*(7), 447. https://doi.org/10.3390/metabo11070447

Zhang, Y., Montgomery, D., White, C. F., Richards, J. G., Brauner, C. J. Farrell, A. P. (2022) Supplementary table deposition-Characterizing the hypoxic performance of a fish using a new metric: P_{AAS}-50 https://doi.org/10.6084/m9.figshare.19658568.v2

Figures

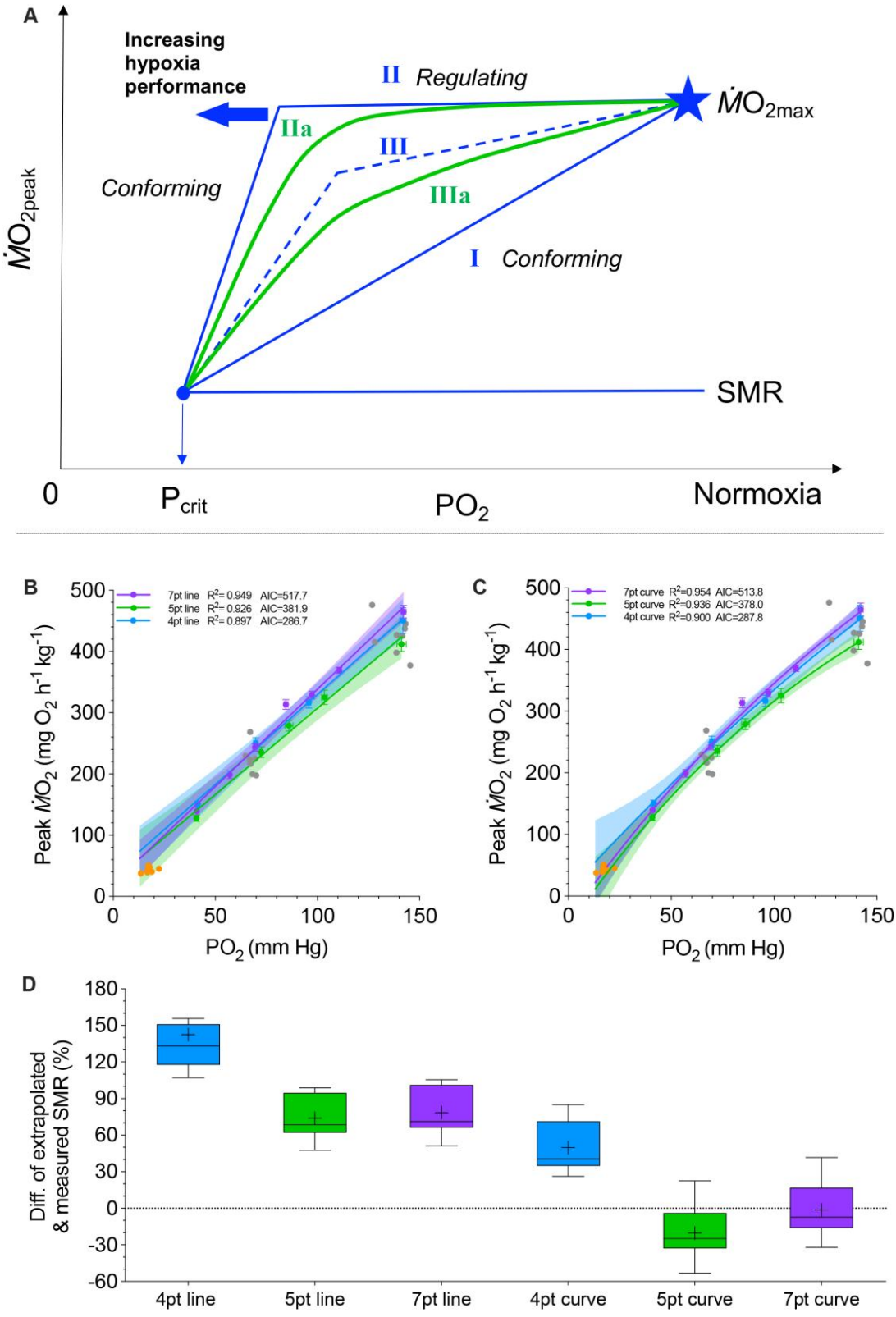

Fig 1. Theoretical hypoxic performance models (A). Three types of models are presented for the relationship between exercised-induced peak oxygen uptake ($\dot{M}O_{2peak}$) and the ambient oxygen partial pressure (PO_2). The maximum oxygen uptake ($\dot{M}O_{2max}$) and standard metabolic rate (SMR) are reference framework. The details of the models are in the Introduction and Fig. S1. Panel B & C are $\dot{M}O_{2peak}$ values (each point is mean ± s.e.m.) for rainbow trout (*Oncorhynchus mykiss*) with independent data sets for the 4-point (4-pt, n=7), the 5-point (5-pt, n=8) and the 7-point (7-pt, n=8) testing protocols. These data were statistically modeled (line equals mean and shade equals 95% C.I.) with either a linear regression model (B) or an asymptotic model (curvilinear fit) (C) (*see* Table S2 in Zhang *et al*., 2022 for all equations). As reference points, independent control measurements of individual P_{crit} and $\dot{M}O_{2min}$ values are in orange and independently measured values for individual $\dot{M}O_{2max}$ and $\dot{M}O_{2peak}$ in naïve fish are in grey. Panel D summarizes as a percentage difference the deviation between the measured $\dot{M}O_{2min}$ in the control fish (mean of the orange symbols) and an estimated values obtained by extrapolating both the linear (B) and curvilinear (C) LOC models for the three different data sets (bar = 25–75 percentile; whiskers = min–max; line = median; plus = mean).

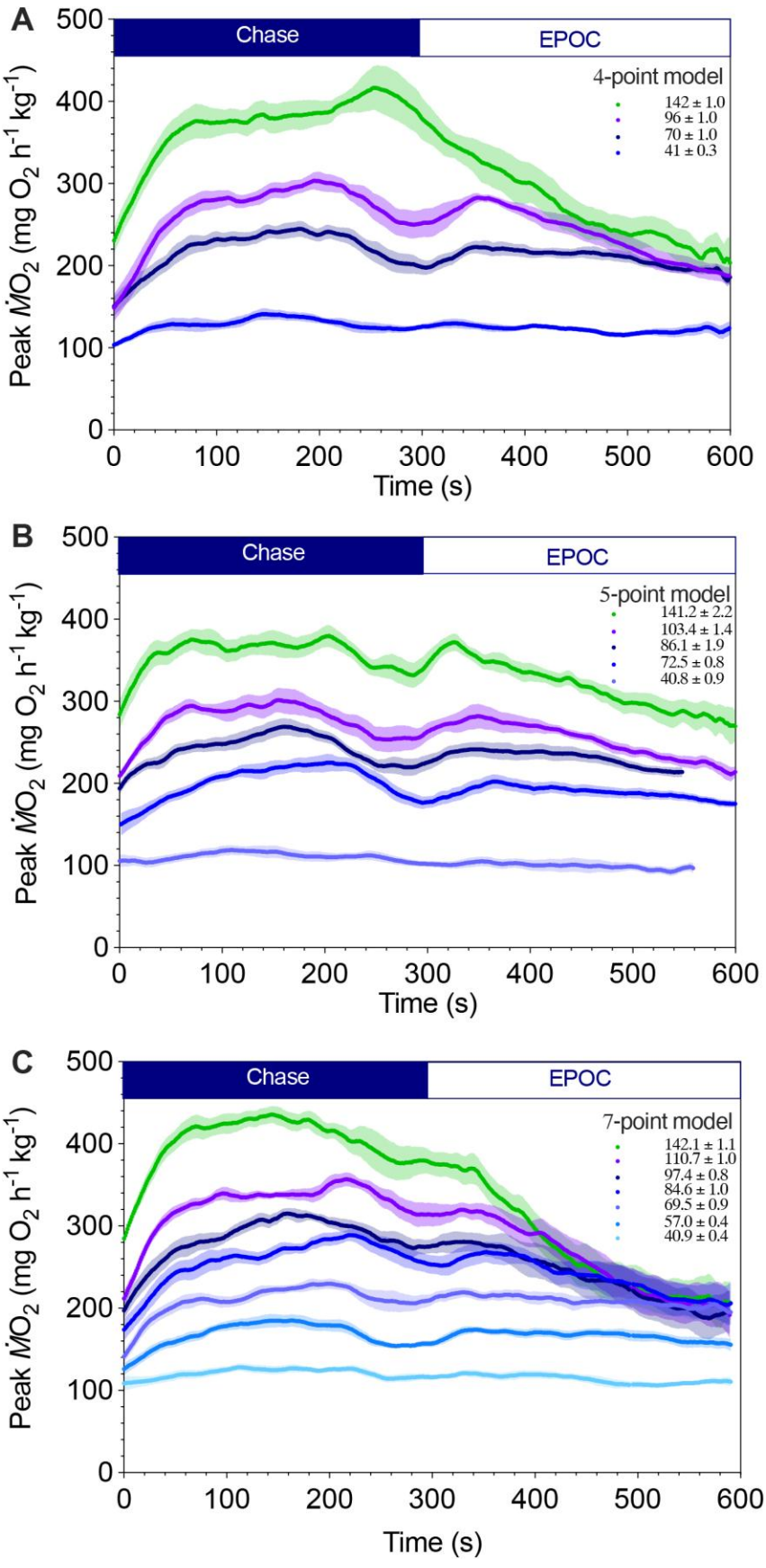

Fig. 2. Continuous peak oxygen uptake ($\dot{M}O_{2peak}$) of rainbow trout (*Oncorhynchus mykiss*) during a chasing and recovery periods, and as a function of ambient oxygen partial pressure (PO_2) (The figure inset provides details on the mean $PO_2 \pm$ s.e.m.) to illustrate both the sustained nature of $\dot{M}O_{2peak}$ while chasing a rainbow trout and the constraint placed upon $\dot{M}O_{2peak}$ by decreasing PO_2. At progressively lower PO_2 values and with suitable recovery periods in between, $\dot{M}O_{2peak}$ was monitored while a fish was chased inside the respirometer for 300 s and during the ensuing 300-s excess post-exercise oxygen consumption (EPOC). Each coloured line represents the mean $\dot{M}O_{2peak}$ at a given PO_2 and each shading represents s.e.m..

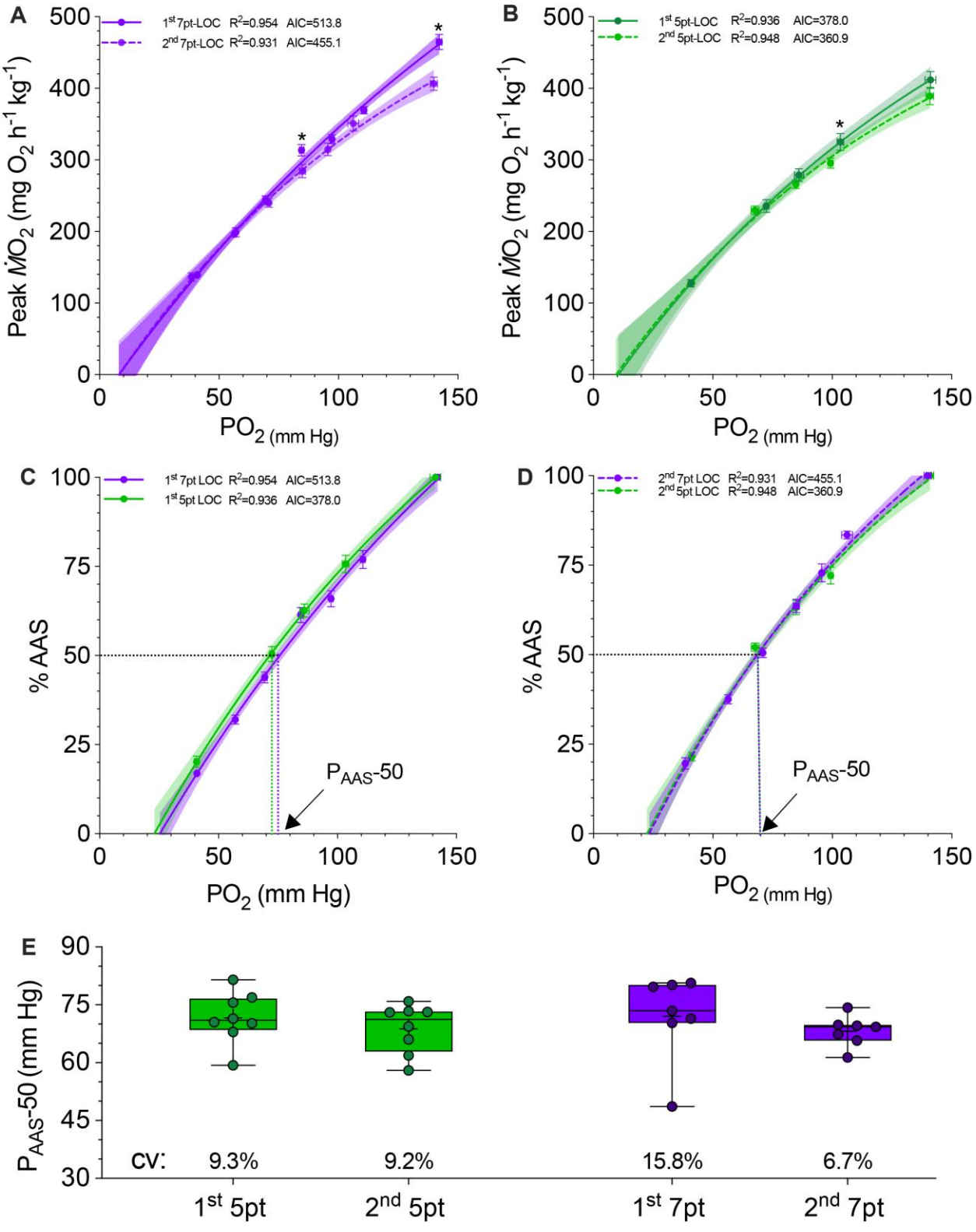

Fig. 3. The reproducibility of the hypoxic performance curve. The same rainbow trout (*Oncorhynchus mykiss*) were measured for either 7-point (7pt, A) or 5-point hypoxic performance curve (5pt, B). Peak oxygen uptake ($\dot{M}O_{2peak}$) and ambient oxygen partial pressure (PO_2) were fitted by asymptotic association equations (line equals mean and shade equals 95% C.I.). The reproducibility was tested on the difference of $\dot{M}O_{2peak}$ values at the similar PO_2 range (Asterisk denoted $\alpha < 0.05$ by paired t-tests) and the three parameters (*i.e.* asymptote, rate constant for a hyperbolic increase, and intercept) in nonlinear mixed-effects model (*see* Table S3 in Zhang *et al*., 2022) (A, B). The $\dot{M}O_{2peak}$ values were normalized to a percentage of the absolute aerobic scope (AAS) of the same individual to derive the minimum PO_2 at which the fish generates 50% of its absolute aerobic scope (P_{AAS}-50) in the 1st (C) and the 2nd tests (D). The P_{AAS}-50 derived from each individual were summarized in bar and whisker plots (bar = 25–75 percentile, whiskers = min–max, line = median, plus = mean) with the coefficient of variation (CV) (E).

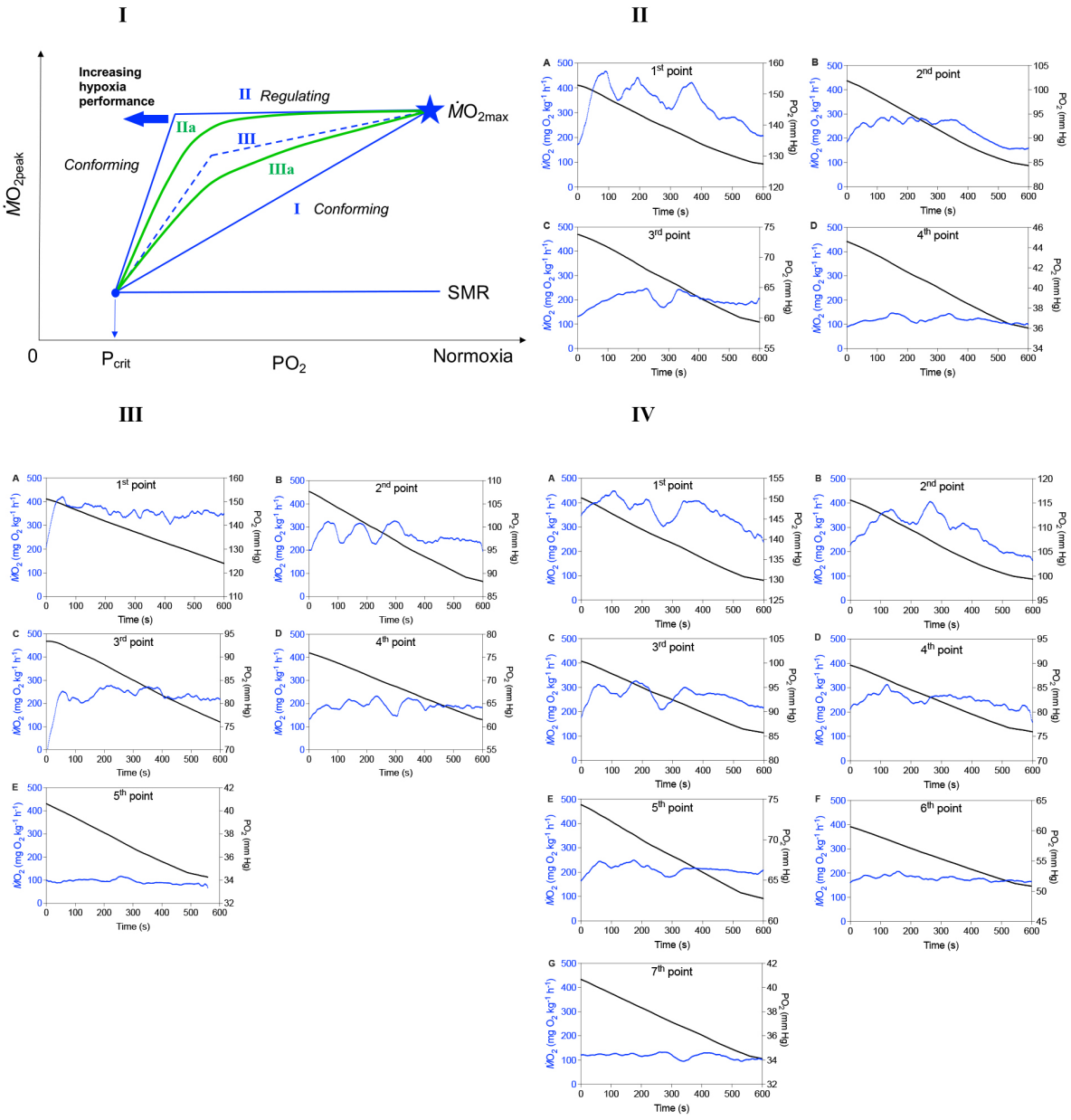

Fig. S1. The detailed elucidation of hypoxic performance models (section I). Model I represent a scenario when a fish regulates $\dot{M}O_{2peak}$ at $\dot{M}O_{2max}$ until a threshold PO_2 is reached, below which $\dot{M}O_{2peak}$ declines linearly to converge with $\dot{M}O_{2min}$ at a critical PO_2 (P_{crit}). Model Ia is a variation on Model I where the transition from the regulating to the conforming states is more gradual. Model II represents a linear conformity of $\dot{M}O_{2peak}$ with ambient PO_2. Model III presents two different phases of linear conformity with ambient PO_2 where $\dot{M}O_{2peak} < \dot{M}O_{2max}$ except in normoxia and a threshold PO_2 exists. Model IIIa represents a curvilinear relationship between $\dot{M}O_{2peak}$ between normoxia and P_{crit}, which is a variation on Model III but one where conformation with ambient increases progressively rather than abruptly with ambient PO_2. To demonstrate the measurements of each point used for model hypoxic performance curve, we showed the representative examples of off-line, continuous analysis of oxygen uptake ($\dot{M}O_2$, blue lines) for an individual rainbow trout (*Oncorhynchus mykiss*) during a 300-s chase inside a respirometer and during the ensuing 300-s recovery period (section II: 4-point model, section III: 5-point model, section IV: 7-point model). Panel A in each section shows the chase in normoxia and the other panels in the same section show the progressively lower ambient dissolved water oxygen levels for the same fish to illustrate that peak oxygen uptake ($\dot{M}O_{2peak}$) can be reached multiple times during the chase and sometimes, but not always, immediately after the chase and that is constrained by progressive hypoxia. All $\dot{M}O_{2peak}$ values were determined on individual fish using an iterative algorithm that coupled a rolling regression analysis and a reliable minimum duration for the sampling window (100 s, *see* analysis in Fig. S2). Since the respirometer remained closed for the entire 600-s recording period, the corresponding decline in the dissolved oxygen level (black lines) that was used to calculate $\dot{M}O_2$ is also shown on the same time axis.

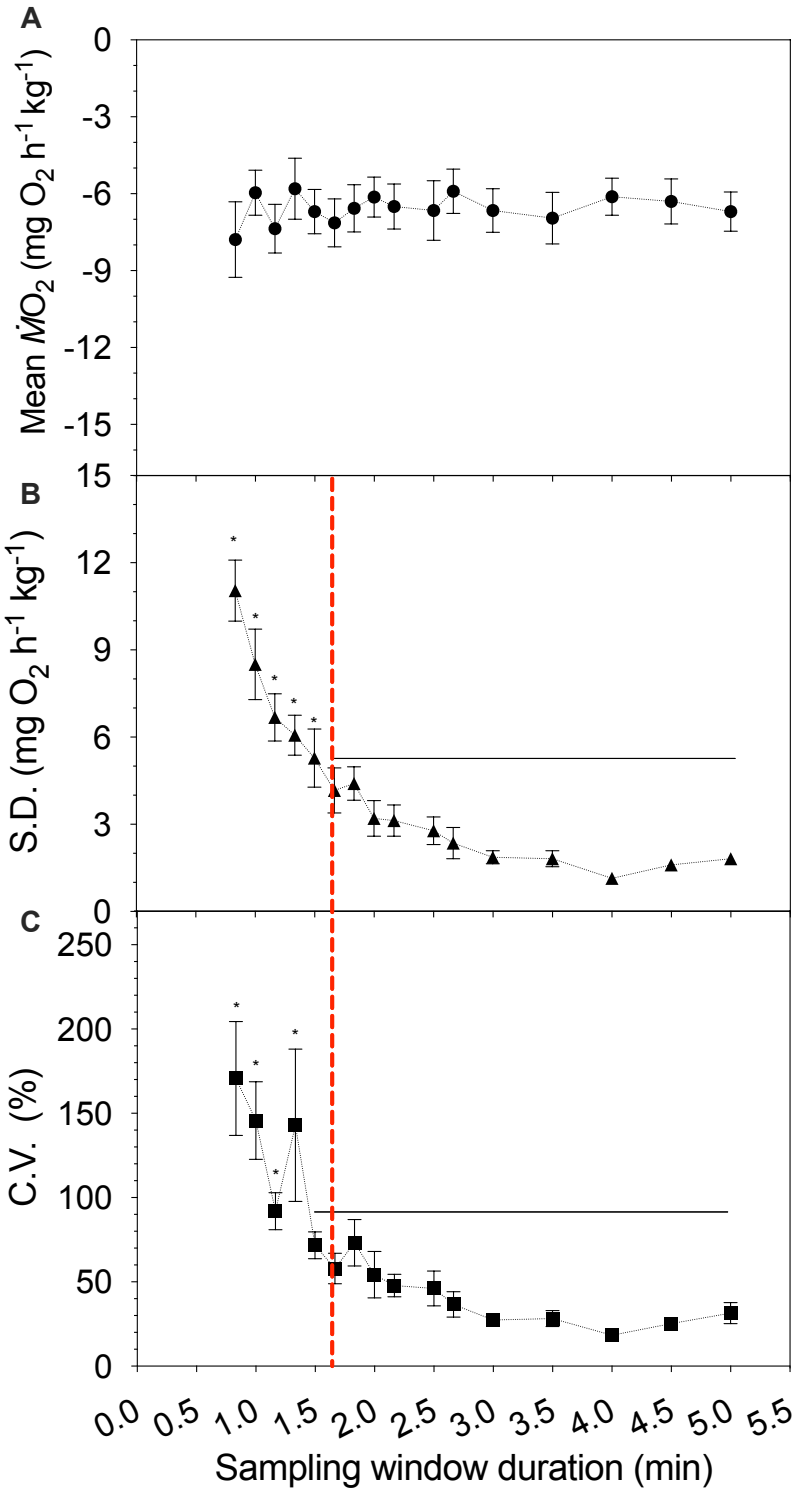

Fig. S2. An analysis of the impact of varying the duration of the sampling window when making an estimate of the rate of oxygen uptake ($\dot{M}O_2$). Traces for constant background $\dot{M}O_2$ (A) of an empty respirometer at 16 ˚C (20-min in total duration; n=8) were used to analyze the signal ($\dot{M}O_2$)-to-noise (statistical variation) ratio. Both (B) standard deviation (S.D.) and (C) coefficient of variation (C.V.) used as estimates of the statistical variation (noise associated with a constant $\dot{M}O_2$ signal) by compiling mean $\dot{M}O_2$ and its statistics from the eight $\dot{M}O_2$ traces as a function of sampling window duration. The S.D. and C.V. values for each sampling window duration were compared using a one-way ANOVA with Tukey's *post-hoc* tests ($\alpha < 0.05$). All values are presented as mean ± s.e.m.. The criterion for selecting minimum duration for the sampling window was the duration prior to a statistical increase in either the S.D. or C.V. of the mean $\dot{M}O_2$ which did not necessarily change from a stable value with longer sampling window durations. This minimum duration proved to be 100 s (vertical red dashed line) although a numerical increase in the mean value seemed to begin with a sampling window duration of <180 s.

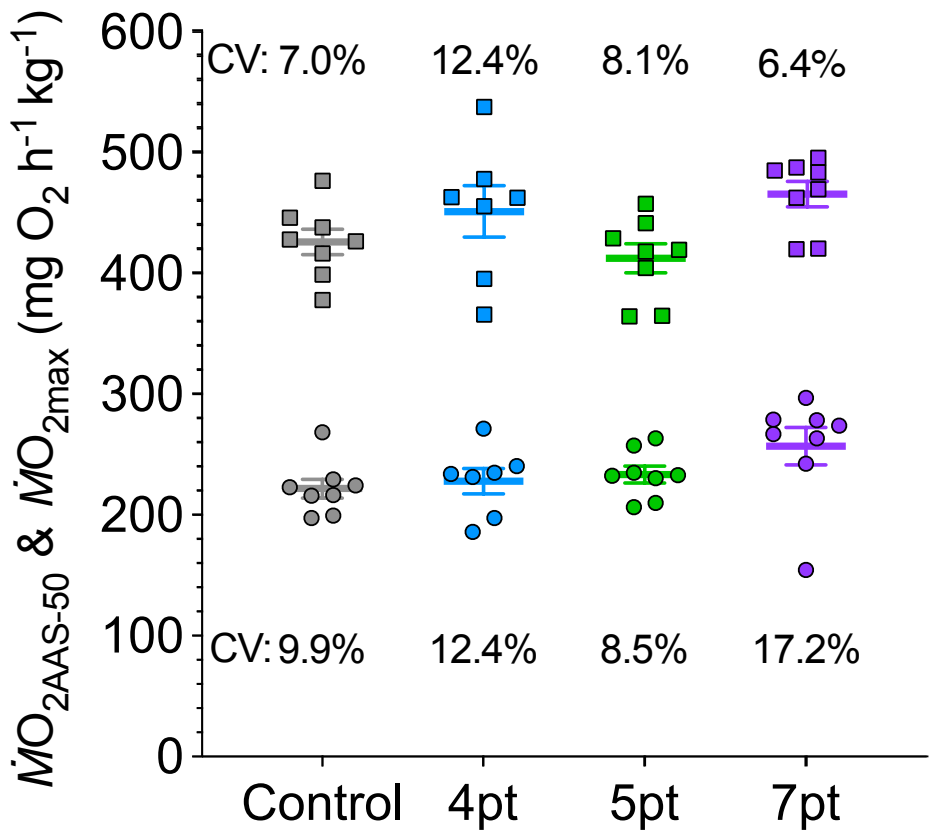

Fig. S3. A comparison of mean (± s.e.m.) peak oxygen uptake at the 50% of absolute aerobic scope ($\dot{M}O_{2AAS-50}$) and mean maximum oxygen uptake ($\dot{M}O_{2max}$) among the three different experimental designs: four-point (4 pt), five-point (5 pt) and seven-point (7 pt) levels of progressive hypoxia. There was not statistical significance (one-way ANOVA Holm-Šídák's *post-hoc* tests). Coefficient of variation (CV) for these mean values are given and the individual values for $\dot{M}O_{2AAS-50}$ (circles) and $\dot{M}O_{2max}$ (squares) for each test group are also shown.